

Systemic and Local CC Chemokines Production in a Murine Model of Infection

Bubonja, Marina; Wraber, Branka; Brumini, Gordana; Gobin, Ivana; Veljković, Danijela; Abram, Maja

Source / Izvornik: **Mediators of Inflammation, 2006, 2006, 1 - 8**

Journal article, Published version

Rad u časopisu, Objavljena verzija rada (izdavačev PDF)

<https://doi.org/10.1155/MI/2006/54202>

Permanent link / Trajna poveznica: <https://urn.nsk.hr/urn:nbn:hr:184:206777>

Rights / Prava: [Attribution 4.0 International](#)/[Imenovanje 4.0 međunarodna](#)

Download date / Datum preuzimanja: **2024-05-10**



Repository / Repozitorij:

[Repository of the University of Rijeka, Faculty of Medicine - FMRI Repository](#)



Research Communication

Systemic and Local CC Chemokines Production in a Murine Model of *Listeria monocytogenes* Infection

Marina Bubonja,¹ Branka Wraber,² Gordana Brumini,³ Ivana Gobin,¹ Danijela Veljkovic,¹ and Maja Abram¹

¹ Department of Microbiology, Medical Faculty, University of Rijeka, 51000 Rijeka, Croatia

² Institute of Microbiology and Immunology, Medical Faculty, University of Ljubljana, 1000 Ljubljana, Slovenia

³ Department of Medical Informatics, Medical Faculty, University of Rijeka, 51000 Rijeka, Croatia

Received 29 December 2005; Revised 17 February 2006; Accepted 19 February 2006

Repeated intragastric inoculation of *Listeria monocytogenes* into BALB/c mice resulted in prolonged bacteraemia and severe hepatic infection. Bacteria could also be isolated from the brain tissue of all experimental mice. During the inflammatory process, chemokine concentrations typically increased at the local site in comparison to the systemic level. The liver-to-serum ratio was more pronounced in the case of macrophage inflammatory protein 1 α (MIP-1 α), suggesting its role in the inflammatory response in the liver. The ratio of brain-to-serum concentration of monocyte chemoattractant protein 1 (MCP-1) remained the same as in the control animals, while it was lower in the infected mice, both in the case MIP-1 α and in the case of regulated on activation, normal T cell expressed and secreted (RANTES). This is in correlation with slight inflammatory infiltrates found in the brain tissue early in infection.

Copyright © 2006 Marina Bubonja et al. This is an open access article distributed under the Creative Commons Attribution License, which permits unrestricted use, distribution, and reproduction in any medium, provided the original work is properly cited.

INTRODUCTION

Listeria monocytogenes infection via the digestive system after consumption of contaminated food is currently thought to be the main source of human listeriosis. Ingestion of *L. monocytogenes* is a very common occurrence, since it is widely distributed in the environment and in many food products [1]. The bacterium is resistant to various environmental conditions such as high salt or acidity, low oxygen conditions, and refrigeration temperatures. Even when *L. monocytogenes* is initially present at a low level in contaminated food, the microorganism can multiply during storage. However, the actual infectious dose of *L. monocytogenes* for human infection continues to be a matter of debate. In healthy adults, listeriosis usually remains a mild or subclinical illness, although febrile gastroenteritis may also occur [2–4]. However, in pregnant women and their foetuses, the elderly, and persons with a weakened immune system, listeriosis is often a fatal infection with sepsis and meningitis/meningoencephalitis being the predominant clinical manifestations.

The murine model of listeriosis has yielded a considerable insight into bacterial virulence factors, pathogenesis of disease, and host-parasite interactions [5]. As a facultative

intracellular pathogen, *L. monocytogenes* evokes a strong T-cell-mediated immune response in infected animals [6, 7] and elicits a production of various soluble mediators, among them cytokines and chemokines [8, 9]. Chemoattractant cytokines or chemokines are a growing group of small, low-weight molecules that are believed to control the nature and magnitude of inflammatory cell infiltration. Because of their vast biological functions they are linked to the pathogenesis of many seemingly unrelated diseases like cancer, atherosclerosis, autoimmune diseases, various microbial infections and so forth [10, 11]. However, the precise role of chemokines is still not fully recognised. It has been reported recently that some of the chemokines, like macrophage inflammatory protein alpha/beta (MIP-1 α / β) and regulated on activation, normal T cell expressed and secreted (RANTES) act together with IFN- γ as type 1 cytokines, [12] while monocyte chemoattractant protein 1 (MCP-1) is a crucial factor for the development of adaptive Th2 responses [13, 14].

In an attempt to obtain a model resembling natural listeriosis, in the present study we explored the course of infection in BALB/c mice following intragastric (ig) inoculation of *L. monocytogenes*. In order to evaluate the contribution of CCchemokines in vivo, the levels of MIP-1 α , MCP-1, and

RANTES were determined by enzyme-linked immunosorbent assay (ELISA) in murine organ homogenates and compared to chemokine levels in the sera drawn from the same animals.

MATERIALS AND METHODS

Bacterial strain

The haemolytic EGD strain (serovar1/2a) of *L monocytogenes* was grown in brain heart infusion (BHI) broth (Difco Laboratories, Detroit, Mich, USA) at 37° C for 24 hours. The culture broth was centrifuged at 3000 × g for 5 minutes, and the pelleted bacteria were resuspended in bicarbonate buffered saline (BBS), pH 6.9. The optical density of the bacterial suspension was estimated using a spectrophotometer at 550 nm, and the numbers of colony-forming units (CFU) of *L monocytogenes* were extrapolated from a standard growth curve. The actual number of CFU in the inoculum was verified by plating on blood agar.

Animals and assay of infection

BALB/c (H2-d haplotype) male mice aged 6–8 weeks were obtained from the breeding colony at the Medical Faculty, University of Rijeka. They were kept in plastic cages and given standard laboratory food and water ad libitum. The experiments were conducted according to the guidelines contained in the International Guiding Principles for Biomedical Research Involving Animals. The Ethical Committee at the University of Rijeka approved all the animal experiments described here.

After overnight fasting, mice (20 animals per group) were challenged with a single dose of 3×10^5 , 3×10^7 , 3×10^8 , 3×10^{10} , or 3×10^{11} viable *L monocytogenes* in a total volume of 0.3 mL BBS, by gastric intubation through a thin vinyl tube connected to a gauge needle. The sixth group was inoculated in the same way with 3×10^7 bacteria but the procedure was repeated during three consecutive days. The control group received only BBS via the same route and in the same manner. Extreme care was taken not to injure the animals during ig inoculation; no animals were used in which there was suspicion of injury or inhalation of the inoculum.

Bacterial counts in organs

At various time intervals, mice were euthanised by CO₂ inhalation, and their livers, spleens, kidneys, and brains (5 mice per group) were dissected and homogenised in 5 mL of sterile phosphate-buffered saline (PBS, pH 7.4). Serial ten-fold dilutions of the organ homogenates were plated on blood agar plates, incubated at 37° C for 24 hours, after which CFU were counted. Bacterial titres are expressed as log₁₀ of CFU per organ.

Histopathological examination

For histopathology, the organs were dissected, fixed in 10% formaldehyde, and embedded in paraffin. Sections (6 µm

thick) were stained with haematoxylin and eosin (H&E). For immunohistochemistry, the paraffine sections were treated using an indirect immunoperoxidase protocol with polyclonal rabbit anti-*L monocytogenes* antiserum (Difco Laboratories, Detroit, Mich, USA) as primary and goat anti-rabbit IgG F(ab')₂ fragments as secondary antibodies. Coloured slides were analysed using a light microscope at 100- and 1000-fold magnification.

Measurement of aminotransferase and chemokine levels

At different time points after bacterial inoculation, the animals (5 mice per group) were anaesthetised with ketamine hydrochloride and blood samples were obtained from the retroorbital plexus. The tubes were centrifuged and the sera were stored at –20° C until analysed. Serum samples were diluted 1 : 5 with distilled water and aspartat aminotransferase (AST) and alanine aminotransferase (ALT) activities were determined using the Clinical Chemistry System Olympus AU 800.

The livers, spleens, kidneys, and brains were aseptically removed, weighed, and frozen in liquid nitrogen and stored at –80° C. Frozen tissue samples were thawed on ice and homogenised in ice-cold PBS (5 mL PBS per 1 g of tissue) with a hand-held tissue homogeniser, and centrifuged at 13 000 × g for 10 minutes at 4° C to precipitate debris as a pellet. Concentrations of MIP-1α, MCP-1, and RANTES were determined in sera and organ supernatants by using Quantikine M immunoassay kits purchased from R&D Systems (Wiesbaden, Germany). Assays were performed according to the manufacturer's instructions and results reported as picogram (pg) of chemokine per mL of tissue homogenate or serum. The detection limit for MIP-1α was 1.5 pg mL^{–1} and for MCP-1 and RANTES it was 2 pg mL^{–1}, respectively. All tests were performed in duplicate.

Statistical analysis

The data for bacterial load, aminotransferase, and chemokine levels are expressed as median values ± interquartile range (IQR). The results obtained from control and experimental groups were compared using the Mann-Whitney test. A statistically significant difference was defined at a *P* value < .05.

RESULTS

Determination of the optimal dose for ig infection

BALB/c mice were inoculated intragastrically with different doses of *L monocytogenes*. As seen in Figure 1 all animals infected with the highest dose of bacteria (3×10^{11} CFU) died within two days of infection. Low survival rate and death of 75% of infected animals was seen in the group receiving 3×10^{10} CFU. After inoculation of 3×10^8 CFU, 50% of the animals succumbed (LD₅₀ for ig route of application), while the majority of mice infected with the lower doses (3×10^7 , 3×10^5 CFU) survived the infection. None of the models seemed

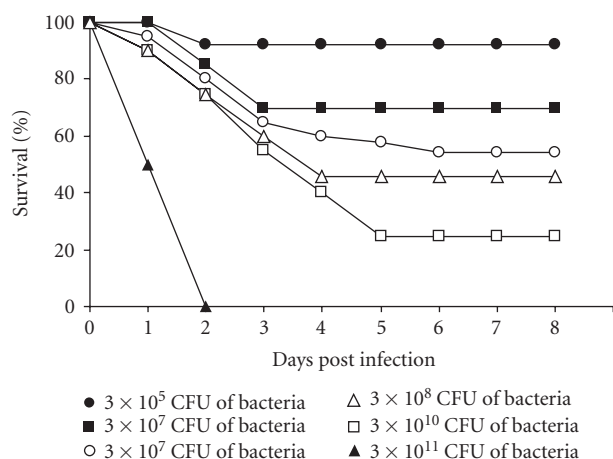


FIGURE 1: Survival of mice infected with different doses of *L monocytogenes*. Mice (20 per group) were infected with single doses of 3×10^{11} (▲), 3×10^{10} (□), 3×10^8 (△), 3×10^7 (■), and 3×10^5 (●) CFU of bacteria. Dose of 3×10^7 (○) was administered repeatedly during three consecutive days.

to be suitable for following the course of ig listeriosis, because animals challenged with high single doses quickly succumbed as a result of the infection, while the tissue changes in mice challenged with lower doses varied widely (data not shown).

In subsequent experiments we applied 3×10^7 CFU for three consecutive days in an attempt to obtain, approximately, the effect of LD₅₀. However, the cumulative dose resulted in a prolonged survival of animals (Figure 1) when compared with the group infected with the single LD₅₀ dose. The infection was highly reproducible.

Course of *L monocytogenes* infection after repeated ig administration

The course of infection was followed for 10 days after administration of the third dose. Infected mice manifested a diarrhoea and visible signs of disease from the first day after receiving the last dose of bacteria. Histopathological examination of the gastric tissue did not reveal inflammatory lesions but changes were seen in the intestinal mucosa. In the villi of the jejunum (Figure 2(a)), as well as in the cecum, prominent oedema of the lamina propria with rare infiltrated plasma cells and macrophages was detected. The duration of these findings was limited and they gradually disappeared from day 3 postinfection (pi). However, in all animals the systemic infection was confirmed by positive blood cultures and isolation of *L monocytogenes* from different organs. Bacteraemia persisted from 2 to 5 days, respectively. To avoid the possibility that CFU recovered from the organ homogenates, especially from the brain tissue, was from the bloodstream rather than from the parenchyma per se, mice were perfused with saline before the organs were removed. Hepatic and splenic infection aggravated during the first days of infection. Maximal CFU per liver and spleen was reached on day 2 or 3

pi, decreasing thereafter (Figure 3). The high bacterial load in the liver corresponded to the histopathological changes. Even on day 7 pi, multiple inflammatory foci, sometimes including central necrosis (Figure 2(b)), could be found in the liver. In antilisteria immunostained sections of the liver tissue, short rods of *L monocytogenes* were easily detected (Figure 2(c)). They usually appeared in clusters, having a tendency to spread towards the healthy surrounding. Elevated levels of AST and ALT in the serum (Figure 4) confirmed severe metabolic liver dysfunction. Congestion and inflammation foci were the main histopathological findings in the spleens of infected mice. Despite of the relatively high number of bacteria isolated from the infected kidneys (Figure 3), we could not find any major tissue damage in the paraffin sections. Surprisingly, *L monocytogenes* was isolated from the brain of all infected animals. Although the bacterial titres did not exceed 10^3 per mL tissue homogenates, it seemed that bacteria had a tendency to increase in number towards the end of the experimental period (Figure 3). This is in concordance with the lack of histological signs of inflammation in the brain tissue during the early phase of infection. However, from day 7 pi, changes appeared mostly as focal infiltration of monocytes in the brain tissue of some infected mice (Figure 2(d)).

Systemic and local concentrations of chemokines

The impact of *L monocytogenes* infection on the CC chemokines milieu in the liver, spleen, and brain tissue was studied and compared with the chemokine pattern in the same organs of noninfected mice. Additionally, the gradient between a local (organ) compartment and the intravascular space was quantified by determining the ratio between the organ and serum levels of MIP-1 α , MCP-1, and RANTES.

In the organs as well as in the sera of noninfected animals, low physiological levels of all measured chemokines were detectable (Figure 5). Baseline levels for all three chemokines were the highest in the spleen and lowest in the brain tissue. In the noninfected brain tissue the most pronounced chemokine was found to be MCP-1, while in the other organs and in the serum, it was RANTES.

In the sera (Figure 5) of infected mice MCP-1 was found to have much higher titres in comparison to RANTES, while MIP-1 α was nearly at the detection level. When compared with the control serum titres, the most pronounced increase was noticed in the case of MCP-1.

During the inflammatory process, a more profound increase in the concentration of chemokines was detected at the local site of inflammation in comparison to the systemic level. In the infected liver (Figure 5) high concentrations of MCP-1 and RANTES were detected, while the MIP-1 α levels were much lower. In the same manner as in the noninfected animals, the highest levels of the measured chemokines in *L monocytogenes*-infected mice were detected in their spleens (Figure 5). MIP-1 α and MCP-1 levels were significantly increased in comparison to the control, which has not been noticed in the case of RANTES. Infection with *L monocytogenes* resulted in increased concentrations of all the measured

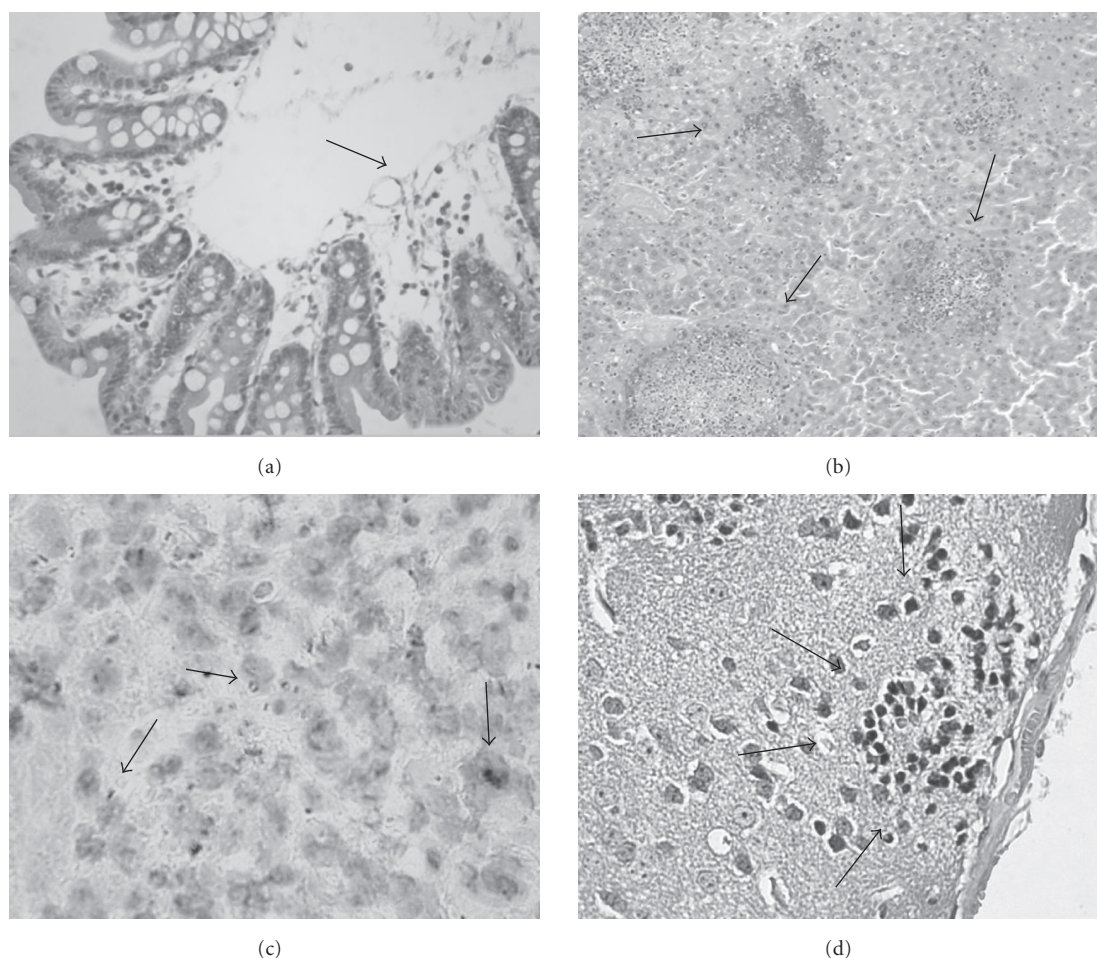


FIGURE 2: Photomicrographs of different tissues of mice infected during three consecutive days with dose of 3×10^7 CFU *L. monocytogenes*. (a) Jejunum; oedema in the lamina propria with infiltrated plasma cells and macrophages at day 2 pi; magnification $\times 400$, H&E staining. (b) Liver tissue; arrows indicate numerous foci of inflammation with central necrosis at day 7 pi; magnification $\times 100$, H&E staining. (c) Liver tissue; arrows point to sporadic rods as well as cluster of *L. monocytogenes* present in the infiltrates at day 3 pi magnification $\times 1000$, anti-*L. monocytogenes* immunostaining. (d) Brain tissue; focal infiltration of monocytes (arrows) at day 7 pi; magnification $\times 400$, H&E staining.

chemokines in the brain tissue. However, only the increase in the titre of MCP-1 was significant in comparison with the noninfected mice.

The chemokine concentration gradient between the tissue and blood regulates the recruitment of inflammatory cells to the site of inflammation, modulating the host response to infection. Wishing to contribute to the understanding of this mechanism, we determined the liver-, spleen-, and brain-to-serum ratios of the tested chemokines (Table 1). In *L. monocytogenes*-infected mice the calculated liver-to-serum ratio was increased, particularly in the case of MIP-1 α , suggesting its possible role in the necroinflammatory response in the liver. The ratio of spleen-to-serum MIP-1 α was about four-fold and MCP-1 about three-fold higher in comparison to the gradient in noninfected spleen tissue. Surprisingly, in the brain tissue of infected animals, the ratio of organ-to-serum concentrations of MCP-1 remained the same as in the control animals, while the ratio was lower in the infected animals, both in the case of MIP-1 α and RANTES.

DISCUSSION

Listeriosis is a serious disease acquired by consumption of contaminated foods. Ingested *L. monocytogenes* traverses from the intestinal wall [15] resulting in systemic infection with meningitis being the predominant clinical manifestation. How the microorganisms get access to the brain tissue is controversial. Some investigators have shown that *L. monocytogenes* can invade neurons and that intra-axonal transport is possible [16]. Ruminants may get infected through the trigeminal nerve after infection of the oral mucosa [17]. Haematogenous dissemination is also possible since *L. monocytogenes* is known to be able to invade endothelial cells [18] and could hence be able to invade through the brain microvasculature. It has been published that central nervous system (CNS) invasion is highly dependent on the level and duration of bacteraemia [19].

In our experimental model it was clearly seen that intragastric administration of *L. monocytogenes* led to development of systemic infection. However, high challenge doses

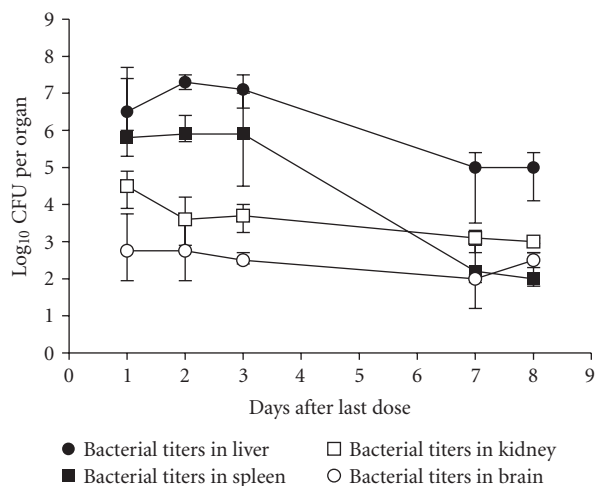


FIGURE 3: Kinetics of bacterial clearance in the organs of mice ig infected during three consecutive days with dose of 3×10^7 CFU *L. monocytogenes*. Bacterial titers in liver (●), spleen (■), kidney (□), and brain (○) were determined at various time points postinfection. Data represent median \log_{10} CFU per organ \pm IQR derived from five mice per time point.

resulted in severe illness and a lethal outcome within 2–5 days pi. Obviously, in this short period there was not enough time for meningitis development and the animals die in overwhelming sepsis. Low inoculation doses also resulted in systemic infection, documented by bacteria isolated from different organs, but the results varied widely. However, when lower doses were applied repeatedly for three consecutive days, a prolonged low-level bacteraemia occurred and *L. monocytogenes* was isolated from the liver, spleen, and kidneys, as well as, from the brain tissue of all infected mice. These data provide support for the hypothesis that not only a high single dose, but also prolonged daily consumption of a low number of *L. monocytogenes* can be hazardous. This is in accordance with the publication of Majjala et al who recently described an outbreak of human listeriosis caused by a prolonged daily consumption of contaminated butter during hospitalization [20].

When BALB/c mice received repeated ig doses of *L. monocytogenes*, the gastroenteric symptoms were manifested as diarrhoea and enteritis was histologically confirmed. Additionally, an acute hepatitis developed with severe histopathological changes and elevated levels of serum aminotransferases. Despite the recovery of substantial numbers of bacteria from the brain homogenates of all infected mice, histological analysis revealed only discrete inflammatory lesions, which appeared in some mice from day 7 pi. Since the number of bacteria in the brain tissue increased towards the end of the experimental period, more severe changes could be expected later in the course of infection. Mounting evidences support the notion that chemokines play an important role in innate immunity to bacteria. Even more, most infectious diseases are characterised by a particular chemokines pattern. Chemokines are synthesised in response to bacterial

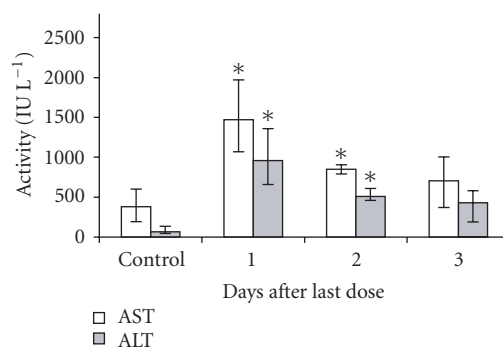


FIGURE 4: Levels of serum aminotransferases of mice ig infected with *L. monocytogenes*. Data represent median values \pm IQR. * $P < .05$ compared to control.

products and cytokines secreted by a wide variety of immune and inflammatory cells, as well as, epithelial and endothelial cells. Knowledge concerning chemokines production during the course of *L. monocytogenes* infection is limited. We investigated the production of three CC-chemokines: MIP-1 α , MCP-1, and RANTES, which are included in the subfamily of inflammatory chemokines. These chemokines are constitutively produced in different murine tissues and sera under physiologic conditions. Upon infection with *L. monocytogenes*, the concentration of these chemokines increased in the circulation, but the increase was more pronounced in the infected organs. Chemokines, like most cytokines, act locally rather than systemically, so these results were not unexpected. Elevated systemic chemokine levels may be required to recruit leucocytes from the circulation. However, once in the extravascular space, leucocyte migration depends on the chemical gradient of chemotactic factors generated within the inflamed tissue. In this sense, the ratio of local-to-systemic chemokine concentration, rather than the absolute tissue or serum values, regulates the biological response. The major target organ of systemic *L. monocytogenes* infection is the liver, where leucocytes are rapidly recruited. During the course of infection, all the analysed CC chemokines were released in the liver. However, the calculated liver-to-serum ratio was significantly increased only in the case of MIP-1 α , suggesting its key role on the influx of inflammatory cells during *L. monocytogenes* infection. In a similar manner, the spleen-to-serum ratio was most pronounced in the case of MIP-1 α , followed to a less extent by MCP-1, while RANTES failed to create a significantly high chemotactic gradient. The role of chemokines in the CNS infections is not well understood. Chemokines have been implicated in a variety of normal CNS functions, although more evidence supports their role in CNS disease and injury [21]. High levels of MIP-1 α , MCP-1, and RANTES were found in the cerebrospinal fluid (CSF) of patients with herpes simplex encephalitis [22]. The same chemokines are shown to be involved in the infiltration of leucocytes into the murine brain after parasitic invasion [23]. Furthermore, significantly elevated concentrations of MCP-1 and MIP-1 α , but not of RANTES, were found in the CSF of patients with acute

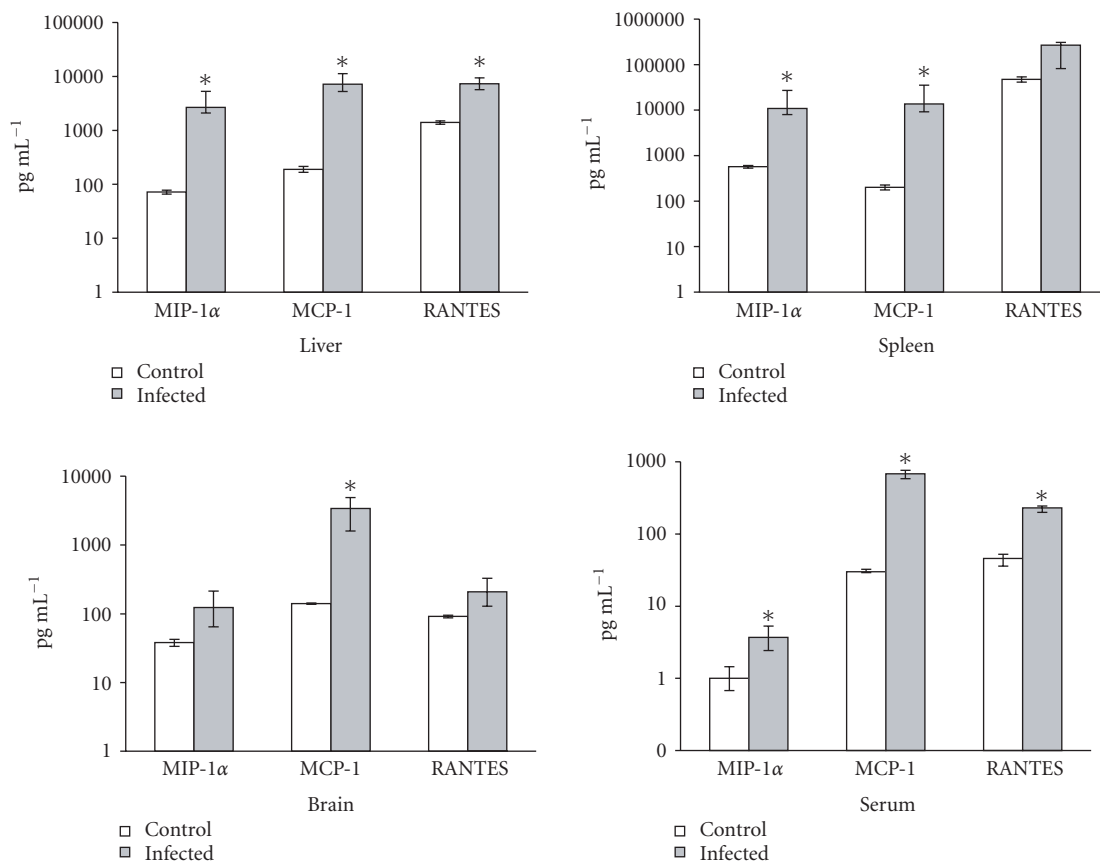


FIGURE 5: Chemokine concentrations in the liver, spleen, brain, and serum. Chemokines were measured by ELISA at day three postinfection in organ homogenates and sera of mice infected with *L. monocytogenes*. Data represent median values \pm IQR and are plotted on logarithmic scales. * $P < .05$ compared to control.

TABLE 1: Local-to-systemic ratio of chemokine levels in control and *L. monocytogenes*-infected mice. Chemokines were measured by ELISA at day three postinfection in organ homogenates and sera of mice infected with *L. monocytogenes*. Data represent the median values and the ranges of chemokine levels. Organ-to-serum ratios were calculated using the median chemokine values for individual organ and serum data.

	Chemokine	Median concentration (range) in pg mL ⁻¹		Ratio (organ : serum)	
		Control	Infected	Control	Infected
Liver	MIP-1α	72.3 (60.5–82)	2660 (380–8105)	72	719*
	MCP-1	190 (145–230)	7180 (1025–26970)	6	11
	RANTES	1400 (1199–1605)	7295 (3390–30525)	30	32
Spleen	MIP-1α	567 (490–645)	10097 (6270–61 800)	567	2729*
	MCP-1	200 (149–252)	13690 (8030–70900)	7	20*
	RANTES	47368 (35330–59650)	257650 (57000–439900)	1032	1120
Brain	MIP-1α	37 (29–47)	123 (26–406)	37	33
	MCP-1	140 (134–146)	3400 (157–17 500)	5	5
	RANTES	91 (82–100)	209 (47–575)	2	< 1
Serum	MIP-1α	1 (0.1–6)	3.7 (0.8–6.7)		
	MCP-1	30 (26.5–39)	683 (220–1218)		
	RANTES	45.9 (27–66.3)	230 (145–323)		

* $P < .05$ compared to control.

bacterial meningitis [24]. In our experimental model, slight increase in concentrations of all measured chemokines was detected in the brain tissue homogenates of *L. monocytogenes*-infected mice, but only MCP-1 concentration increased significantly. However, the brain to serum MCP-1 ratio did not differ in comparison to the noninfected animals. In the case of MIP-1 α and RANTES the brain-to-serum ratio was found to be even lower in the infected than in the control mice. This lack of significant chemokines gradient was paralleled with the lack of visible brain tissue changes in early stages of experimental infection. Possible explanations for this absence of MIP-1 α and RANTES brain-to-serum gradients may be their high systemic levels and the lack of infiltrated cells in the brain tissue, sources of these chemokines. It has been shown that MIP-1 α and RANTES were produced in the brain tissue by infiltrating leucocytes, whereas MCP-1 was produced by resident glial cells [25, 26]. So, among these analysed CC chemokines, MCP-1, perhaps with the other chemotactic factors, may contribute to the recruitment of monocytes noticed one week pi in the brain tissue of infected mice. In the light of production of MCP-1 in other acute brain diseases [27, 28], this chemokine seems to play a fundamental role in the host response to brain injury.

Many of these findings are in agreement with the results of other authors and do support their hypotheses concerning the possible mechanisms involved in the pathogenesis of *L. monocytogenes* infection. However, some results open new and unanswered questions concerning the role of chemokines and inflammatory cells that they recruit during this complex systemic infection. Finally, we can also conclude that the used experimental model has shown to be very promising in the study of this important food-borne disease.

ACKNOWLEDGMENTS

The authors thank Professor Dr Hrvoje Gomercic, Department of Anatomy, Histology and Embryology, Veterinary Faculty, University of Zagreb, Croatia, for pathohistological analyses. This work was supported by a grant (0062023) from the Ministry of Science, Education and Sports, Croatia.

REFERENCES

- [1] Schlech WF III. Foodborne listeriosis. *Clinical Infectious Diseases*. 2000;31(3):770–775.
- [2] Dalton CB, Austin CC, Sobel J, et al. An outbreak of gastroenteritis and fever due to *Listeria monocytogenes* in milk. *New England Journal of Medicine*. 1997;336(2):100–105.
- [3] Aureli P, Fiorucci GC, Caroli D, et al. An outbreak of febrile gastroenteritis associated with corn contaminated by *Listeria monocytogenes*. *New England Journal of Medicine*. 2000;342(17):1236–1241.
- [4] Hof H. *Listeria monocytogenes*: a causative agent of gastroenteritis? *European Journal of Clinical Microbiology and Infectious Diseases*. 2001;20(6):369–373.
- [5] Abram M, Schluter D, Vuckovic D, Wraber B, Doric M, Deckert M. Murine model of pregnancy-associated *Listeria monocytogenes* infection. *FEMS Immunology and Medical Microbiology*. 2003;35(3):177–182.
- [6] Dunn PL, North RJ. Resolution of primary murine listeriosis and acquired resistance to lethal secondary infection can be mediated predominantly by Thy-1+ CD4- CD8- cells. *Journal of Infectious Diseases*. 1991;164(5):869–877.
- [7] Lara-Tejero M, Pamer EG. T cell responses to *Listeria monocytogenes*. *Current Opinion in Microbiology*. 2004;7(1):45–50.
- [8] Abram M, Schluter D, Vuckovic D, Wraber B, Doric M, Deckert M. Effects of pregnancy-associated *Listeria monocytogenes* infection: necrotizing hepatitis due to impaired maternal immune response and significantly increased abortion rate. *Virchows Archiv*. 2002;441(4):368–379.
- [9] Abram M, Vuckovic D, Wraber B, Doric M. Plasma cytokine response in mice with bacterial infection. *Mediators of Inflammation*. 2000;9(5):229–234.
- [10] Rollins BJ. Chemokines. *Blood*. 1997;90:909–928.
- [11] Chensue SW. Molecular machinations: chemokine signals in host-pathogen interactions. *Clinical Microbiology Reviews*. 2001;14(4):821–835.
- [12] Dorner BG, Scheffold A, Rolph MS, et al. MIP-1 α , MIP-1 β , RANTES, and ATAC/lymphotactin function together with IFN- γ as type 1 cytokines. *Proceedings of the National Academy of Sciences of the United States of America*. 2002;99(9):6181–6186.
- [13] Gu L, Tseng S, Horner RM, Tam C, Loda M, Rollins BJ. Control of TH2 polarization by the chemokine monocyte chemoattractant protein-1. *Nature*. 2000;404(6776):407–411.
- [14] Huang D, Wang J, Kivisakk P, Rollins BJ, Ransohoff RM. Absence of monocyte chemoattractant protein 1 in mice leads to decreased local macrophage recruitment and antigen-specific T helper cell type 1 immune response in experimental autoimmune encephalomyelitis. *Journal of Experimental Medicine*. 2001;193(6):713–725.
- [15] Havell EA, Beretich GR Jr, Carter PB. The mucosal phase of *Listeria* infection. *Immunobiology*. 1999;201(2):164–177.
- [16] Jin Y, Dons L, Kristensson K, Rottenberg ME. Neural route of cerebral *Listeria monocytogenes* murine infection: role of immune response mechanisms in controlling bacterial neuroinvasion. *Infection and Immunity*. 2001;69(2):1093–1100.
- [17] Otter A, Blakemore WF. Observation on the presence of *Listeria monocytogenes* in axons. *Acta Microbiologica Hungarica*. 1989;36(2-3):125–131.
- [18] Greiffenberg L, Goebel W, Kim KS, Daniels J, Kuhn M. Interaction of *Listeria monocytogenes* with human brain microvascular endothelial cells: an electron microscopic study. *Infection and Immunity*. 2000;68(6):3275–3279.
- [19] Berche P. Bacteremia is required for invasion of the murine central nervous system by *Listeria monocytogenes*. *Microbial Pathogenesis*. 1995;18(5):323–336.
- [20] Majjala R, Lyytikäinen O, Autio T, Aalto T, Haavisto L, Honkanen-Buzalski T. Exposure of *Listeria monocytogenes* within an epidemic caused by butter in Finland. *International Journal of Food Microbiology*. 2001;70(1-2):97–102.
- [21] Karpus WJ. Chemokines and central nervous system disorders. *Journal of Neurovirology*. 2001;7(6):493–500.
- [22] Rosler A, Pohl M, Braune HJ, Oertel WH, Gerns D, Sprenger H. Time course of chemokines in the cerebrospinal fluid and serum during herpes simplex type 1 encephalitis. *Journal of the Neurological Sciences*. 1998;157(1):82–89.
- [23] Cardona AE, Gonzalez PA, Teale JM. CC chemokines mediate leukocyte trafficking into the central nervous system during murine neurocysticercosis: role of $\gamma\delta$ T cells in amplification of the host immune response. *Infection and Immunity*. 2003;71(5):2634–2642.

- [24] Spanaus KS, Nadal D, Pfister HW, et al. C-X-C and C-C chemokines are expressed in the cerebrospinal fluid in bacterial meningitis and mediate chemotactic activity on the cerebrospinal fluid in bacterial meningitis and mediate chemotactic activity on peripheral blood-derived polymorphonuclear and mononuclear cells in vitro. *Journal of Immunology*. 1997;158(4):1956–1964.
- [25] Glabinski AR, Balasingam V, Tani M, et al. Chemokine monocyte chemoattractant protein-1 is expressed by astrocytes after mechanical injury to the brain. *Journal of Immunology*. 1996;156(11):4363–4368.
- [26] Miyagishi R, Kikuchi S, Takayama C, Inoue Y, Tashiro K. Identification of cell types producing RANTES, MIP-1 alpha and MIP-1 beta in rat experimental autoimmune encephalomyelitis by in situ hybridization. *Journal of Neuroimmunology*. 1997;77:17–26.
- [27] Kim JS. Cytokines and adhesion molecules in stroke and related diseases. *Journal of the Neurological Sciences*. 1996;137(2):69–78.
- [28] Lahrtz F, Piali L, Spanaus KS, Seebach J, Fontana A. Chemokines and chemotaxis of leukocytes in infectious meningitis. *Journal of Neuroimmunology*. 1998;85(1):33–43.

